

A One-Pot Approach to the Preparation of Organic Core–Shell Nanoobjects with Different Morphologies

Huisheng Peng, Daoyong Chen,* and Ming Jiang

Department of Macromolecular Science and The Key Laboratory of Molecular Engineering of Polymers, Fudan University, Shanghai 200433, China

Received November 18, 2004

Revised Manuscript Received February 21, 2005

Organic core–shell nanoobjects have attracted much attention due to their great potential in both applied and theoretical research fields.^{1–3} Generally speaking, the core–shell nanoobjects, especially these with morphologies other than spheres, are prepared through self-assembly of block copolymers.^{4–6}

Recently, we found that in the common solvent of a block copolymer (i.e., the block copolymer is molecularly dispersed in the solvent) cross-linking one of the blocks directly would lead to the formation of core–shell nanospheres.⁷ When the repulsion between shells of the formed core–shell nanospheres is enough to localize the cross-linking reaction, the regular nanospheres are the final product. The repulsion between the arms of star polymers is also indispensable for preparation of regular star polymers using an “arm first” approach (the as-prepared star polymers are actually core–shell nanospheres⁸). It should be noted that, in these two cases, there is a possibility for the cores of the resultant core–shell nanospheres to couple with each other due to the reaction between the cores.^{8,9} Two extreme results were reported: when the repulsion between the shells, which depends on the density and length of the shell-forming arms, provides enough protection for the reactive cores, regular core–shell nanospheres are yielded; when the protection is insufficient, irregular aggregates or precipitates are produced (Scheme 1).

Here we report an approach to synthesize core–shell nanoobjects other than core–shell nanospheres with high efficiency through the coupling between the cores of core–shell nanospheres, which are produced by a one-pot anionic polymerization. The core–core coupling controlled by the shell–shell repulsion that varies during the coupling is suggested to explain the formation of the fiberlike and the graftlike nanoobjects.

Under strictly oxygen-free and anhydrous conditions, living polystyrene chains prepared by an anionic polymerization initiated by *n*-butyllithium, capped with 1,1-dibenzylethylene, were added with a mixture of divinylbenzene (DVB) and 4-vinylpyridine (4VP) in THF at $-78\text{ }^{\circ}\text{C}$ (compositions of the reactants are presented in Table 1). The reactions were kept for more than 10 h, and the resultant solutions were precipitated by *n*-hexane and further purified to obtain white powders. Grams of powders can be obtained from 100 mL of solution. The white powders were readily redissolved in DMF and characterized by dynamic light scattering (DLS) and electron microscopy (SEM and TEM). The DLS results are presented in Table 1.

DLS data suggest that the aggregates produced in systems 1 and 2 are nanospheres with a narrow size

Scheme 1. When the Cores Are Rigid and Can React with Each Other, They Will Be Either Isolated (a) or Coupled with Each Other To Form Irregular Aggregates or Precipitates (b)

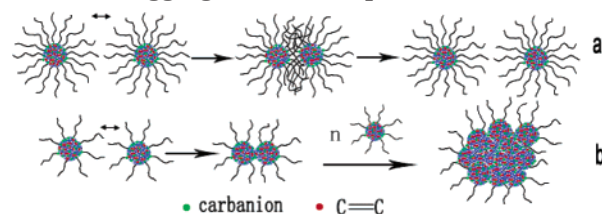


Table 1. Composition, Sizes, and Size Distributions of the Resultant Nanoobjects

system no.	$M_{w,PS}^a$	PDI_{PS}^b	N_{4VP}/N_{St}^c	N_{DVB}/N_{4VP}^d	$\langle R_h \rangle$ (nm) ^e	PDI_{DLS}^f
1	90 281	1.12	1.04	1/9	66	0.09
2	114 520	1.23	1.41	1/9	111	0.09
3	80 622	1.03	3.21	1/9	78	1.00
4	84 244	1.10	4.61	1/9	95	1.00
5	8 213	1.18	3.00	1/9	217	1.00

^a Molecular weight of polystyrene macroinitiator. ^b Polydispersity index of polystyrene macroinitiator. ^c Molar ratio of styrene units of the PS macroinitiator to 4-vinylpyridine (4VP). ^d Molar ratio of divinylbenzene (DVB) to 4VP. ^e Average hydrodynamic radius of the nanoobjects measured by dynamic laser scattering (DLS). ^f Polydispersity index of the size distribution measured by DLS.¹⁰

distribution, since the polydispersity index (PDI_{DLS}) of $\langle R_h \rangle$ is as low as 0.09 (Table 1). This is proved by SEM and TEM observations (Figure 1a,b). DLS measurements of the products from systems 3–5, however, show that the PDI_{DLS} values are as high as 1.00, and $\langle R_h \rangle$ values of the aggregates remarkably depend on the scattering angles (measured between 30° and 120° , data not shown).¹¹ These results are consistent with the fiberlike morphology of the aggregates formed in system 3 (Figure 1c–e; Figure 1d demonstrates that when the solution was concentrated, some nanofibers were piled together during the drying of the solution on the copper grids for TEM observations; however, the outline of the individual fibers is clearly seen) and system 4 (Figure 1f,g) and the graftlike morphology of the aggregates yielded in system 5 (Figure 1h,i), based on SEM and TEM observations.

The nanoobjects without staining are invisible in the TEM images. While after reacting with CH_3I in DMF, they are clearly shown in the TEM images. It is demonstrated in each of the images shown in Figure 1a–g that the diameter of the spheres or the width of the nanofibers is uniform. However, the width of the nanofibers or the diameter of the nanospheres observed by TEM is remarkably less than that of the same nanoobjects by SEM (the details are given as a note¹²). This remarkable difference indicates the core–shell structure.⁷ The core visible in TEM images after staining with CH_3I should be composed of pyridine groups, whereas the shell undetected by TEM but observed by SEM should be formed by PS.⁷ This core–shell structure of the nanoobjects is supported by X-ray photoelectron spectroscopy (XPS) analysis, which probes several nanometers in depth of the samples surfaces, as the content of nitrogen atoms detected by XPS is almost zero.

* Corresponding author. E-mail: chendy@fudan.edu.cn.

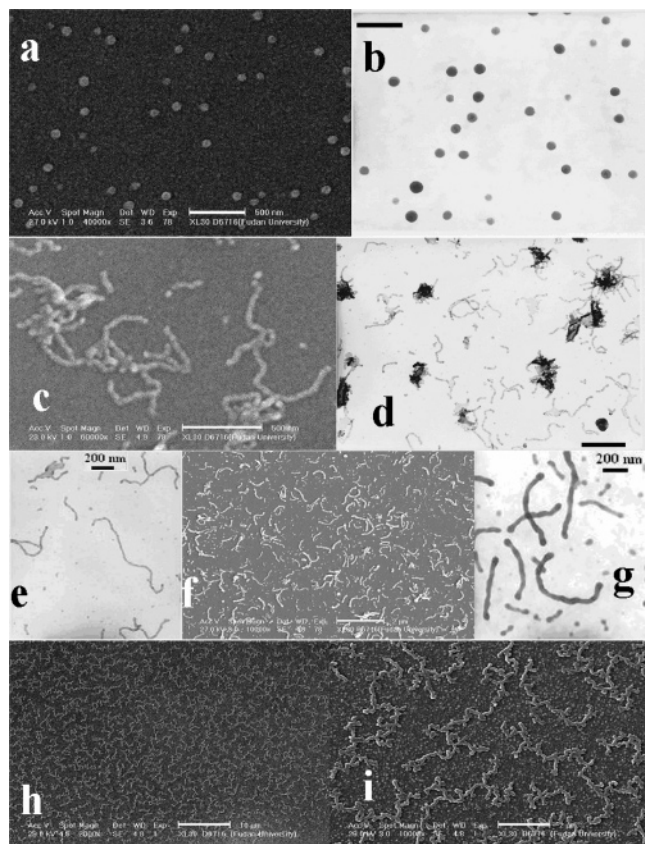


Figure 1. Electron microscopy images of the nanoobjects: a (SEM) and b (TEM): nanospheres produced from system 1; c (SEM), d and e (TEM): nanofibers produced from system 3; f (SEM) and g (TEM): nanofibers produced from system 4; h and i: SEM images of the graftlike aggregates produced from system 5. The scale bars in a, b, c, d, e, f, g, h, and i are 500, 200, 500, 500, 200, 2000, 200, 10000, and 2000 nm, respectively.

It is noted in the SEM and TEM images that the nanofibers or nanografts coexist with nanospheres. The nanofibers show evidences of connected nanospheres with the width of the nanofibers being close to the diameter of the coexisting nanospheres. It is reported that, during preparation of star polymers using the arm first approach, longer reaction time resulted in an increasing amount of particle–particle coupling.⁸ This conclusion is consistent with our study. We characterized the aggregates produced from these systems at the reaction times of 1 and 10 h, respectively. It is proved that at 1 h reaction time the monomer 4VP and the cross-linker DVB were exhausted, and almost only spherical aggregates were formed. However, at 10 h reaction time, fiberlike aggregates were obtained from systems 3 and 4 and graftlike ones from system 5. In addition, the sizes and the size polydispersity indexes of the aggregates obtained at 10 h reaction time are remarkably larger than those of the aggregates produced in the respective systems (3, 4, and 5) at 1 h reaction time. These facts demonstrate that the nanofibers and the nanografts are produced by the reaction coupling between the preformed core–shell nanospheres. The question is: how can the reaction coupling between the cores lead to such regular core–shell nanoobjects?

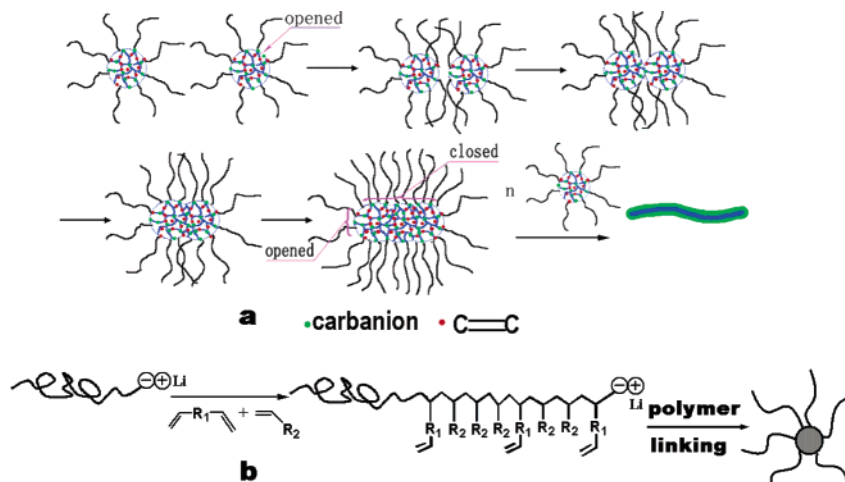
The TEM and SEM observations indicate that after the coupling of core–shell nanospheres forming a fiber their cores become sections of a cylinder. So, the cores

have to deform from a spherical shape to cylindrical one, indicating that the flexibility of them is necessary in forming the nanofibers. In the reported studies, the molar ratio of cross-linker to the core-forming monomer is higher than 25%, so the core of the resultant star polymers should be rigid. This resulted in two extreme results, as mentioned before. Similarly, in our study, the systems with the values of N_{DVB}/N_{4VP} being higher than 20% lead to nanospheres or irregular aggregates/precipitate as well. Considering the fact that the contact and reaction between the cores must overcome the repulsion between the shells, the length and the density of the shell-forming arms, which depend on $M_{W,PS}$ and the ratio of N_{4VP}/N_{St} (Table 1) and determine the repulsion, are also important. This is consistent with this study as well. When the value of N_{DVB}/N_{4VP} was decreased to 10%, the (relatively) large $M_{W,PS}$ and large N_{St}/N_{4VP} (implicating the long arms with a high density on the surface of the cores) lead to nanospheres (systems 1, 2), the large $M_{W,PS}$ and small N_{St}/N_{4VP} lead to nanofibers (systems 3, 4), and the small $M_{W,PS}$ and small N_{St}/N_{4VP} lead to the formation of nanografts (system 5).

It is well-known that there are two mechanisms governing the aggregation between particles, which are diffusion-limited aggregation (DLA) and the reaction-limited aggregation (RLA).^{13–16} DLA will result in loosely connected clusters with a typical fractal dimension of 1.7–1.8, while RLA leads to a denser cluster with a fractal dimension of 2.0–2.2. The results of this study exhibit that the aggregation between core–shell nanoparticles due to the coupling between the cores can be controlled to produce regular aggregates by controlling the flexibility of the core, the density, and the length of the shell-forming arms. Recently, Lodge et al. reported segmented wormlike aggregates resulting from the aggregation between individual micelles formed by a ABC miktoarm stars.¹⁷ It is stated that in forming a string the different cores are able to share their coronas, thus protecting them from the highly unfavorable exposure to water. It is also a statement in an article by Wooley et al. that for the sphere-to-rod transitions the process requires sphere (micelle) collisions followed by reorganization into smooth cylindrical rods.¹⁸ These statements are inspiring for us to explain the results of this study.

As indicated in Scheme 1a, when the arms are long enough and the density of the arms is high, the contact and the subsequent reaction between the cores can be prohibited. Whereas in the cases that the arms are relatively short and/or with a relatively low density on the cores' surface, when two core–shell nanospheres approach one another, a fluctuation in the density of the arms may lead to the exposure and the coupling of the cores.^{3,17} During the coupling, because of the repulsion between the arms and the low cross-linking density of the cores (which should lead to high flexibility of the cores and the mobility of the arms on the cores' surface), the arms originally within the regions to be connected (i.e., the interface between two connected cores) must largely get away from the connected area and redistribute on the unconnected surface. This is evidenced by the TEM observations. The TEM images of the nanofibers indicate that PS arms were not considerably wrapped. Otherwise, the images of nanofibers should show a segmented morphology since PS chains should have little contrast in the TEM images, as mentioned before. It is imaginable that, after the fusion of a core

Scheme 2. (a) Interstar Reaction between Carbanions (Green Points in the Cores) and Carbon–Carbon Double Bonds (Red Points) Leads to the Star–Star Coupling;^a (b) Schematic Description of the Chemistry Involved in the Formation of a Star Polymer



^a When the cross-linking density of core is low, the core is flexible and shell-forming arms have enough mobility on the core's surface. After the fusion of one core with two other cores, the area indicated as "closed" becomes unreactable, whereas the area "opened" are still reactable; thus, nanofibers are produced.

with two other cores to become a section of a cylinder, the surface area of the core is remarkably decreased. Therefore, nearly all the arms are distributed on the decreased surface. The density of arms on the core must be remarkably increased. We speculate that in the cases when nanofibers are produced, after the densification, the core cannot couple with another core again. So, the core-shell nanofibers are formed in a way similar to the linear oligomerization of a monomer; otherwise, if the densification is not enough to protect further coupling of the core with another core, graftlike nanoaggregates will be produced. This speculation is schematically described in Scheme 2a.

The chemistry involved in the formation of star polymers using arm-first approach has been described in the literature.^{8,19} Initially, in the present case, the macroinitiator (PS-Li⁺) initiates the copolymerization of DVB and 4VP, leading to the production of a short block bearing carbon-carbon double bonds (CCDBs) with a carbanion at the propagating chain end (Scheme 2b). Then, the polymer linking (chain-chain coupling) resulting from the interchain reaction between the carbanions and the CCDBs leads to the formation of core-shell star polymer (Scheme 2b). Actually, at the early stage, the chain-chain coupling should be accompanied by the further addition of DVB and 4VP to the "living" chain ends, which will further increase the possibility of the chain-chain coupling.

The star-star coupling has been reported in many studies as well.^{20,21} The chemical reaction, in the present case, involved in the star-star coupling also occurs between the carbanions and the CCDBs. The ¹H NMR characterization of the final products resulting from the present study indicates that there are still signals (the peaks between 5.0 and 6.0 ppm) associated with unreacted CCDBs of incorporated DVB appearing in the ¹H NMR spectra (in deuterated DMF). Meanwhile, during the reaction, the carbanions exist in each star, and the number of the carbanions in a star is theoretically equal to the number of the arms (PS chains) of the star. Therefore, during the reaction, the carbanions and the CCDBs coexist in the star (the coexistence in a same star is due to the fact that these species are fixed at different positions of a cross-linked structure). The

interstar reaction between the CCDBs and the carbanions leads to the star-star coupling. In addition, it is demonstrated that the resultant stars have a core-shell structure with the linear PS chains as the shell and the copolymer of DVB and 4VP as the core, as mentioned before. Therefore, the unreacted CCDBs of incorporated DVB and the carbanions should be located in the core, and the star-star coupling should occur between the cores of the stars, as indicated in Scheme 2a.

In conclusion, the core-shell structured nanospheres, nanofibers, and nanografts with PS as the shell and the P4VP cross-linked by DVB as the core can be produced with high efficiency. This approach makes use of in-situ coupling of core-shell nanospheres produced by an arm first approach via an anionic polymerization. We believe that the coupling of the cores of core-shell particles can be controlled to synthesize regular nanoobjects other than nanospheres through adjusting the flexibility of the cores, the density, and the length of the shell-forming arms. This work will generate much interest in the fields of polymer physics and chemistry.

Acknowledgment. This work has been supported by the National Science Foundation of China (50273006, 50333010).

References and Notes

- (1) Haag, R. *Angew. Chem., Int. Ed.* **2004**, *43*, 278–282.
- (2) Forster, S.; Plantenberg, T. *Angew. Chem., Int. Ed.* **2002**, *41*, 689–714.
- (3) Jang, J.; Oh, J. H. *Adv. Mater.* **2003**, *15*, 977.
- (4) Jain, S.; Bates, F. S. *Science* **2003**, *300*, 460–464.
- (5) Jenekhe, S. A.; Chen, X. L. *Science* **1998**, *279*, 1903–1907.
- (6) Zhang, L. F.; Yu, K.; Eisenberg, A. *Science* **1996**, *272*, 1777–1779.
- (7) Chen, D. Y.; Peng, H. S.; Jiang, M. *Macromolecules* **2003**, *36*, 2576–2578.
- (8) Xia, J.; Zhang, X.; Matyjaszewski, K. *Macromolecules* **1999**, *32*, 4482.
- (9) Bosman, A. W.; Heumann, A.; Klaerner, G.; Benoit, D.; Frechet, J. M. J.; Hawker, C. J. *J. Am. Chem. Soc.* **2001**, *123*, 6461–6462.
- (10) Chu, B.; Wang, Z. L.; Yu, J. Q. *Macromolecules* **1991**, *24*, 6832–6838.

- (11) Wu, C.; Li, M.; Kwan, S. C. M.; Liu, G. J. *Macromolecules* **1998**, *31*, 7553–7554.
- (12) Note: in Figure 1, the diameter of the spheres: 80–90 nm, based on Figure 1a; 45–55 nm based on Figure 1b. In Figure 2, the width of the nanofibers: 40–50 nm based on Figure 2a; 20–30 nm based on Figure 2b,c. In Figure 3, the width of nanofibers: 75–80 nm based on Figure 3a; 40–50 nm based on Figure 3b.
- (13) Witten, T. A.; Sander, L. M. *Phys. Rev. Lett.* **1981**, *47*, 1400.
- (14) Jullien, R.; Kolb, M. *J. Phys. A* **1984**, *17*, L639.
- (15) Ball, R. C.; Weitz, D. A.; Witten, T. A.; Leyvraz, F. *Phys. Rev. Lett.* **1987**, *58*, 274.
- (16) Cheng, H.; Wu, C.; Winnik, M. A. *Macromolecules* **2004**, *37*, 5127–5129.
- (17) Li, Z. B.; Kesselman, E.; Talmon, Y.; Hillmyer, M. A.; Lodge, T. P. *Science* **2004**, *306*, 98–101.
- (18) Ma, Q. G.; Remsen, E. E.; Clark, C. G.; Kowalewski, T.; Wooley, K. L. *Proc. Natl. Acad. Sci. U.S.A.* **2002**, *99*, 5058–5063.
- (19) Frater, D. J.; Mays, J. W.; Jackson, C. J. *J. Polym. Sci., Part B: Polym. Phys.* **1997**, *35*, 141–151.
- (20) Themistou, E.; Patrickios, C. S. *Macromolecules* **2004**, *37*, 6734–6743.
- (21) Williamson, D. T.; Elman, J. F.; Madison, P. H.; Pasquale, A. J.; Long, T. E. *Macromolecules* **2001**, *34*, 2108–2114.

MA047620V